Key ^{18}Ne(α,p)^{21}Na breakout reaction in x-ray bursts: first experimental determination of spin-parities for α resonances in ^{22}Mg via resonant elastic scattering of ^{21}Na+p

J.J. He[1],* L.Y. Zhang[1,2,3], A. Parikh[4,5], S.W. Xu[1], H. Yamaguchi[6], D. Kahl[6], S. Kubono[1,6,11], J. Hu[1], P. Ma[1], S.Z. Chen[1,3], Y. Wakabayashi[7,11], B.H. Sun[8], H.W. Wang[9], W.D. Tian[9], R.F. Chen[1], B. Guo[10], T. Hashimoto[6], Y. Togano[11], S. Hayakawa[6], T. Teranishi[12], N. Iwasa[13], T. Yamada[13], and T. Komatsubara[14]

[1]*Institute of Modern Physics, Chinese Academy of Sciences, Lanzhou 730000, China*
[2]*School of Nuclear Science and Technology, Lanzhou University, Lanzhou 730000, China*
[3]*University of Chinese Academy of Sciences, Beijing 100049, China*
[4]*Department de Física i Enginyeria Nuclear, EUETIB, Universitat Politècnica de Catalunya, Barcelona E-08036, Spain*
[5]*Institut d'Estudis Espacials de Catalunya, Barcelona E-08034, Spain*
[6]*Center for Nuclear Study, University of Tokyo, RIKEN campus, Wako, Saitama 351-0198, Japan*
[7]*Advanced Science Research Center, Japan Atomic Energy Agency, Ibaraki 319-1106, Japan*
[8]*School of Physics and Nuclear Energy Engineering, Beihang University, Beijing 100191, China*
[9]*Shanghai Institute of Applied Physics, Chinese Academy of Sciences, Shanghai 201800, China*
[10]*China Institute of Atomic Energy, P.O. Box 275(46), Beijing 102413, China*
[11]*RIKEN (The Institute of Physical and Chemical Research), Wako, Saitama 351-0198, Japan*
[12]*Department of Physics, Kyushu University, 6-10-1 Hakozaki, Fukuoka 812-8581, Japan*
[13]*Department of Physics, University of Tohoku, Miyagi 980-8578, Japan and*
[14]*Department of Physics, University of Tsukuba, Ibaraki 305-8571, Japan*

(Dated: January 21, 2013)

The ^{18}Ne(α,p)^{21}Na reaction is thought to be one of the key breakout reactions from the hot CNO cycles to the *rp*-process in type I x-ray bursts. To determine this astrophysical reaction rate, the resonance parameters of the compound nucleus ^{22}Mg have been investigated by measuring the resonant elastic scattering of ^{21}Na+p. An 89 MeV ^{21}Na radioactive ion beam was produced at the CNS Radioactive Ion Beam Separator and bombarded a 8.8 mg/cm^2 thick polyethylene target. The recoiled protons were measured at scattering angles of $\theta_{c.m.}\approx$175° and 152° by three ΔE-E silicon telescopes. The excitation function was obtained with a thick-target method over energies E_x(^{22}Mg)=5.5–9.2 MeV. The resonance parameters have been determined through an R-matrix analysis. For the first time, we have experimentally determined the J^π values for ten states above the α threshold in ^{22}Mg. The ^{18}Ne(α,p)^{21}Na reaction rate has been recalculated, and the astrophysical impact of our new rate has been investigated through one-zone postprocessing x-ray burst calculations. Our new rate significantly affects the peak nuclear energy generation rate and the onset temperature of this breakout reaction in these phenomena.

PACS numbers: 25.60.-t, 23.50.+z, 26.50.+x, 27.30.+t

Type I x-ray bursts (XRBs), one of the most fascinating astrophysical phenomena, are characterized by sudden dramatic increases in luminosity of roughly 10–100 s in duration, with a total energy release of about 10^{39} erg per burst. These recurrent phenomena (on timescales of hours to days) have been the subject of many observational, theoretical and experimental work (for reviews see *e.g.*, [1–3]). The characteristics of XRBs have been surveyed extensively in a number of space-borne x-ray satellite observatory missions, including RXTE, BeppoSAX, Chandra, HETE-2, and XMM/Newton. More than 90 galactic XRBs have been identified since their initial discovery in 1976. These observations have provided abundant data and opened a new era in x-ray astronomy. The bursts have been interpreted as being generated by thermonuclear runaway on the surface of a neutron star that accretes H- and He-rich material from a less evolved companion star in a close binary system [4, 5]. The accreted material burns stably through the hot, β-limited carbon-nitrogen-oxygen (HCNO) [6, 7] cycles, giving rise to the persistent flux. Once critical temperatures and densities are achieved, breakout from this region can occur through, *e.g.*, α-induced reactions on the waiting point nuclei ^{14}O, ^{15}O and ^{18}Ne. Through the rapid proton capture process (rp-process) [8–10], this eventually results in a rapid increase in energy generation (ultimately leading to the XRB) and nucleosynthesis up to A$\sim$100 mass region [11, 12]. Among the breakout reactions, the ^{18}Ne(α,p)^{21}Na reaction may provide the principal breakout route from the HCNO cycle into the rp-process [7]; however, the actual astrophysical conditions under which this occurs depend critically on the actual ^{18}Ne(α,p)^{21}Na thermonuclear rate. In the temperature region of interest for XRBs, this rate has not been sufficiently well determined.

The reaction rate for ^{18}Ne(α,p)^{21}Na is dominated by

*Electronic address: jianjunhe@impcas.ac.cn

the resonance contributions [13]. The uncertainties of current rates are mainly caused by the errors in excitation energies E_x (or resonance energies E_R) and resonance strengths $\omega\gamma$. The first theoretical estimate [13] of this reaction rate was made based on rather limited experimental level-structure information in the compound nucleus ^{22}Mg above the α threshold at 8.142 MeV [14]. After that, the levels in ^{22}Mg have been extensively studied, and more than 40 levels were observed above the α threshold. Such high level-density suggests that a statistical-model approach might provide a reliable estimate of the rate. However, only natural-parity states in ^{22}Mg can be populated by the ^{18}Ne+α channel, and thus the effective level density will be considerably lower. The α-unbound states in ^{22}Mg were previously studied by many transfer reaction experiments. In the ^{12}C(^{16}O,^{6}He)^{22}Mg [15], ^{25}Mg(^{3}He,^{6}He)^{22}Mg [16] and ^{24}Mg(^{4}He,^{6}He)^{22}Mg [17] experiments, the excitation energies in ^{22}Mg were determined with a typical uncertainty of ±20–30 keV. Later on, the excitation energies were determined precisely with unprecedented resolution by a ^{24}Mg(p,t)^{22}Mg [18] experiment, in which the uncertainty was about 1–15 keV for most states above the α threshold. With these precise excitation energies, the uncertainties in ^{18}Ne(α,p)^{21}Na rate can be largely reduced.

The above indirect studies mainly focused on the excitation energies determination, and the spin-parity assignments were not strictly constrained. Some spin-parity assignments were made [13, 15, 18] simply by referring to those of mirror states in ^{22}Ne; such assignments are dubious due to the high level-density in this excitation energy region. In a later ^{24}Mg(p,t)^{22}Mg [19] experiment, several spin-parity assignments were made via an angular distribution measurement. However, the insufficient resolution of their measurements at scattering angles $\theta_{c.m.}$ above 20° makes such J^π assignments questionable [18]. In addition, two new spin-parity assignments were given tentatively in our previous low-statistics experiment [20], and such assignments still need to be confirmed by a high-statistics experiment.

A comparison of all available reaction rates shows discrepancies of up to several orders of magnitude around T∼1 GK [18], and therefore it remains unclear whether the statistical-model calculations provide a reliable rate estimation in a wide temperature region. At present, there are still many resonances (above α threshold) without firm spin-parity assignments, which need to be determined experimentally. As a consequence, the accuracy of the current ^{18}Ne(α,p)^{21}Na reaction rate is mainly limited by the lack of experimental spin-parity and spectroscopic information of the resonances in ^{22}Mg above the α threshold.

Up to now, only two direct measurements for the ^{18}Ne(α,p)^{21}Na reaction have been performed and extended down to the energies of $E_{c.m.}$=2.0 MeV [21] and $E_{c.m.}$=1.7 MeV [22]. These energies are still too high compared with the energy region $E_{c.m.}$≤1.5 MeV of interest for HCNO breakout in XRBs. Exciting results [23] have recently become available at the ISAC II facility at TRIUMF, where the ^{18}Ne(α,p_0)^{21}Na cross section was determined in the energy region of $E_{c.m.}$=1.19–2.57 MeV by measuring the time-reversal reaction ^{21}Na(p,α)^{18}Ne in inverse kinematics. The temperature region of interest in XRBs is about 0.4–2.0 GK, corresponding to a Gamow energy of $E_{c.m.}$=0.5–2.8 MeV for this reaction, *i.e.*, to an excitation region of E_x=8.6–11.0 MeV in ^{22}Mg. Therefore, the recent results [23] are still insufficient for a reliable rate at all temperatures encountered within XRBs.

In this paper, we determine the thermonuclear ^{18}Ne(α,p)^{21}Na rate through a new measurement of the resonant elastic scattering of ^{21}Na+p. In this mechanism, ^{22}Mg is formed via sub-Coulomb barrier fusion of ^{21}Na+p as an excited compound nucleus, whose states promptly decay back into ^{21}Na+p. This process interferes with Coulomb elastic scattering resulting in a characteristic resonance pattern observed in the excitation function [24]. With this approach, the excitation function was obtained simultaneously in a wide energy range of 5.5–9.2 MeV in ^{22}Mg with a well-established thick-target method [25–27], without changing the beam energy. For the first time, we have experimentally determined the J^π values for ten states above the α threshold in ^{22}Mg. The astrophysical impact on the energy generation rate and nucleosynthesis in the XRBs is discussed with our new rates.

In the past ten years, many radioactive ion beams (RIBs) have been successfully produced and separated at CRIB (CNS Radioactive Ion Beam separator) [28, 29] at the Center for Nuclear Study (CNS), University of Tokyo, by using an in-flight method. Most of these RIBs were subsequently used in resonant elastic scattering experiments with a thick-target method [20, 30–33], which proved to be a successful method as being adopted in the present study. For this experiment, some experimental details were preliminarily described elsewhere [36]. An 8.2 MeV/nucleon primary beam of ^{20}Ne^{8+} was accelerated by an AVF cyclotron (K=79) at RIKEN, and bombarded a liquid nitrogen-cooled D_2 gas target (90 K) [34] with an average intensity of 65 pnA. The thickness of D_2 gas was about 2.9 mg/cm^2 at 530 Torr pressure. The ^{21}Na beam was produced via the ^{20}Ne(d,n)^{21}Na reaction in inverse kinematics. After the Wien filter, a purity of 70% for the ^{21}Na beam was achieved on the secondary target.

The arrangement of detectors and targets at the experimental focal plane of CRIB was shown in Fig. 3 in Ref. [36]. Two parallel-plate avalanche counters (PPACs) [35] measured the timing and position of the incoming beam with a position resolution of 1 mm or better. Here, the timing signal was used as part of the event trigger and for particle identification, and the position and incident angle of each beam particle on the target were determined by the two PPACs. The beam impinged on an 8.8 mg/cm^2 polyethylene $(CH_2)_n$ target, which was thick enough to stop all the beam ions. In addition, a 10 mg/cm^2 thick carbon target was used

for evaluating the C background contribution. The ^{21}Na beam bombarded the secondary targets at energy about 89.4 MeV (ΔE=1.9 MeV in FWHM). The averaged beam intensity was about 2×10^5 pps. The beam particles were clearly identified in an event-by-event mode by using the position at PPACb and the TOF between PPACb and the RF signal from the cyclotron [36]. The recoiled light particles were detected with three Micron [37] silicon ΔE-E telescopes centered at angles of $\theta_{\rm Si}$=0°, +14° and -14° with respect to the beam line, respectively. Each ΔE-E telescope subtended an opening angle of about 10° with a solid angle of about 27 msr in the laboratory frame. In the center-of-mass ($c.m.$) frame for elastic scattering, the relevant averaged scattering angles are determined to be $\theta_{c.m.}\approx$175°, 152° and 151°, respectively. The double-sided-strip (16×16 strips) ΔE detectors measured the energy, position and timing signals of the particles, and the pad E detectors measured their residual energies. The recoiled particles were identified by the ΔE-E method, together with a TOF-E method in which timing signals were given by PPACb and ΔE detectors [36]. The energy calibration for the Si detectors was carried out by using secondary proton beams produced with CRIB and a standard triple-α source.

The ^{21}Na+p elastic-scattering excitation functions were reconstructed using the procedure described previously [20, 32]. Figure 1 shows the proton elastic-scattering spectrum for a scattering angle of $\theta_{c.m.}\approx$175°. The cross-section data were corrected for the stopping cross sections of ions in the target [27, 38], and the data within the dead-layer region (between ΔE and E detectors) were removed from the figure. The carbon background contribution, as well as any small contamination of high-energy particles in the cocktail beam not rejected by the veto E detector, were subtracted accordingly using the data taken with the C target. The uncertainties shown are mainly of statistical origin. The excitation energies indicated on Fig. 1 are calculated by a relation of E_x=E_R+Q_p. Here, the resonance energy E_R is determined by an R-matrix analysis (see below), and the proton separation energy Q_p=5.504 MeV is adopted based on the updated masses of ^{21}Na and ^{22}Mg [14, 39]. The corresponding energies adopted in Ref. [18] are also indicated in the figure for comparison, which agree well with ours within the uncertainties.

The ^{21}Na+p excitation function has been analyzed by a multichannel R-matrix [40] code `MULTI` [41]. An overall R-matrix fit is also shown in Fig. 1. A channel radius of R_n=1.35(1+21$^{\frac{1}{3}}$) fm [13, 15] was adopted in the calculation. The successful reproduction of the well-known states [18, 24] at 6.329, 6.587, 6.611, and 6.792 MeV by the code (see Fig. 1) provides confidence in the present method. In this paper, we focus on determining the resonance parameters of those states above the α threshold in ^{22}Mg, which eventually determine the ^{18}Ne(α,p)^{21}Na reaction rate. The resonance parameters for all observed states will be published elsewhere in more detail [42].

In total, ten resonances above the α-threshold were

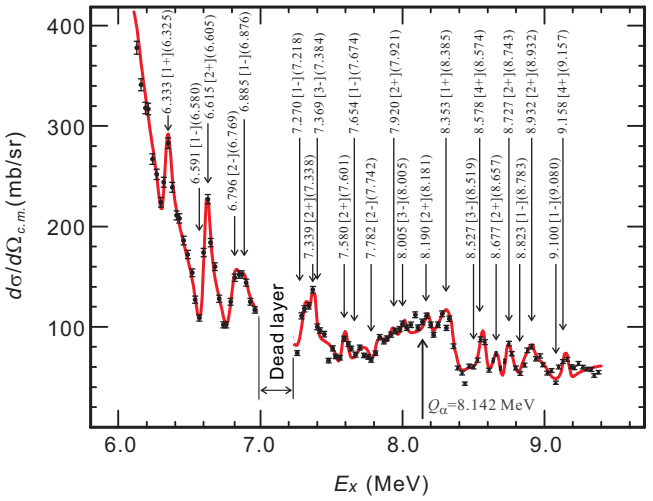

FIG. 1: (Color online) Experimental $c.m.$ differential cross section for resonant elastic scattering of ^{21}Na+p at a scattering angle of $\theta_{c.m.}\approx$175°. It also shows a best overall R-matrix fit. The energies adopted in Ref. [18] are indicated in the parentheses for comparison; the location of α threshold is also shown.

observed and analyzed by the R-matrix code. For the first time, we have experimentally confirmed the J^π values tentatively assigned by Matic *et al.* [18] for seven states at 8.181, 8.519, 8.574, 8.783, 8.932, 9.080 and 9.157 MeV, and assigned here new J^π values for three states at 8.385, 8.657 and 8.743 MeV. As an example, the typical R-matrix fits with possible J^π, channel spin s and orbital angular momentum ℓ for the presently observed 8.578, 8.353, 8.677 and 8.727 MeV states are shown in Fig. 2. The presently observed 8.578 MeV state is closest to the 8.574 MeV in the work of Matic *et al.* in which it was assigned to be a 4^+ state based on a shell-model calculation. As shown in Fig. 2(a), both 2^+ and 4^+ can fit our data very well. As such, our data support the previous 4^+ assignment. The observed 8.353 MeV state is regarded as the 8.385 MeV state of Matic *et al.* whose J^π was suggested to be 2^+ by referring to the mirror state in ^{22}Ne. In addition, we assigned it J^π=(1^+–3^+) in a previous low-statistics experiment [20] where 1^+ was also the most probable assignment. In this work, J^π=1^+ is again the best candidate as shown in Fig. 2(b). Furthermore, this state was only weakly populated in the previous transfer-reaction experiments [15, 17, 18] which preferentially populated the natural-parity states in ^{22}Mg. This supports our assignment of 1^+ unnatural-parity to this state. The observed 8.677 MeV state corresponds to Matic *et al.* 8.657 MeV state, which was assigned as a J^π=0^+ also based on a shell-model calculation. However, such a prediction is questionable because of the high level density at such a high excitation energy region. Matic *et al.* regarded this state as the 8.613 MeV state observed in Ref. [15] where it was assumed to be 3^- by simply shifting the energy of mirror 8.741 MeV state in ^{22}Ne by ∼130 keV. As shown in Fig. 2(c), a J^π=2^+ is now ex-

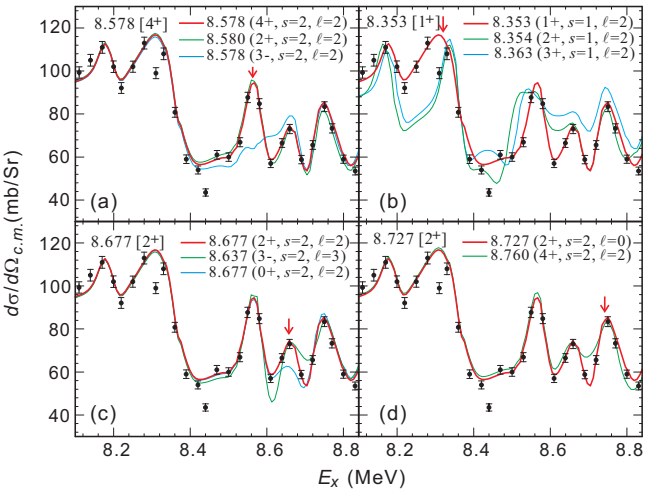

FIG. 2: (Color online) Sample R-matrix fitting results for some resonances above α-threshold. The (red) thicker lines represent the best fits. The relevant channel spin s and orbital angular moment ℓ values are indicated.

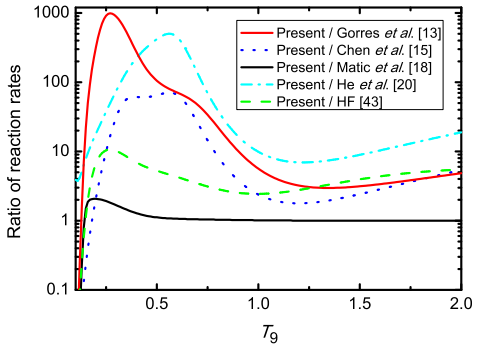

FIG. 3: (Color online) Ratios between present reaction rate and previous ones as a function of temperature.

clusively assigned to this state. The observed 8.727 MeV state is regarded as the Matic *et al.* 8.743 MeV state, which was simply assumed to be the mirror of the 8.976 MeV, 4^+ state in ^{22}Ne. The present R-matrix fit strongly prefers a 2^+ rather than a 4^+ as shown in Fig. 2(d). It is worth mentioning that the data at scattering angle around $\theta_{c.m.}\approx152^\circ$ also support the J^π assignments discussed above [42].

The ^{18}Ne$(\alpha,p)^{21}$Na rate is calculated by a narrow resonance formalism [15, 18]. Part of the resonance parameters for the reaction rate calculations are summarized in Table I. The proton partial widths (Γ_p) deduced from our data will be given elsewhere [42] as here we have calculated the ^{18}Ne$(\alpha,p)^{21}$Na rate assuming $\omega\gamma=\frac{\omega\Gamma_\alpha\Gamma_p}{\Gamma_{\rm tot}}\simeq\omega\Gamma_\alpha$. In this calculation, all resonance energies E_R and strengths $\omega\gamma$ are adopted from the work of Matic *et al.*, except for those states with new J^π values whose strengths are recalculated as listed in Table I. Resonance parameters for states between E_x=8.743–13.010 MeV have been adopted directly from Table VII of Ref. [18] for the present rate calculation. In order to

TABLE I: Part of resonance parameters utilized for the ^{18}Ne$(\alpha,p)^{21}$Na rate calculation. Resonance parameters for states between E_x=8.743–13.010 MeV have been adopted directly from Table VII of Ref. [18] for the present calculation.

$E_x^{\rm Pres.}$ (MeV)	$E_x^{[15]}$ (MeV)	$E_R^{[15]}$ (MeV)	J^π	S_α	Γ_α (eV)	$\omega\gamma$ (MeV)
8.190[a]	8.181	0.039	2^+	0.284	1.70×10^{-65}	8.53×10^{-71}
8.353[b]	8.385		1^+			
8.527[a]	8.519	0.377	3^-	0.004	7.00×10^{-15}	4.87×10^{-20}
8.578[a]	8.574	0.432	4^+	0.06	3.60×10^{-13}	3.26×10^{-18}
8.677[c]	8.657	0.515	2^+	0.32	2.05×10^{-8}	1.03×10^{-13}
8.727[c]	8.743	0.601	2^+	0.11	2.69×10^{-7}	1.34×10^{-12}

[a]All S_α, Γ_α and $\omega\gamma$ values adopted from Ref. [18].
[b]Newly assigned unnatural-parity 1^+ state, no rate contribution.
[c]Recalculated Γ_α and $\omega\gamma$ values based on new J^π assignments.

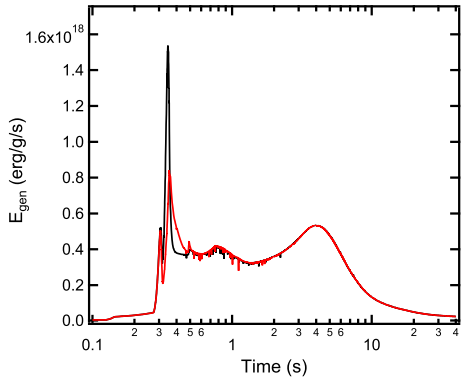

FIG. 4: Nuclear energy generation rates during one-zone XRB calculations using the K04 thermodynamic history [44]. Results using the present rate (black) and Görres *et al.* [13] rate (red) are indicated.

demonstrate the discrepancies between different rates, the ratios between the present rate and the previous ones are shown in Fig. 3. Comparing to the rate of Matic *et al.*, the present rate is much smaller below 0.13 GK, because of the 1^+ character that we have now assigned to the 8.385 MeV state. Consequently, this state does not contribute to the rate due to its unnatural-parity property. On the other hand, the present rate is about 2 times larger around 0.2 GK, because of our new 2^+ assignments for the 8.657 and 8.743 MeV states. Comparing to other available rates [13, 15, 20], our new rate is about a factor of 2–1000 times larger within the temperature region of interest for XRBs. The curve labeled HF is a Hauser-Feshbach statistical-model calculation taken from Ref. [43]. It shows that our new rate and Matic *et al.* rate are about 2–5 times larger than the theoretical prediction beyond 1.0 GK.

The impact of our new ^{18}Ne$(\alpha,p)^{21}$Na rate was examined in the framework of one-zone XRB postprocessing calculations. Three different XRB thermodynamic histories were employed, including the K04 ($T_{\rm peak}$=1.4 GK) and S01 ($T_{\rm peak}$=1.9 GK) models [44, 45], as well as that of the hottest shell in burst 3 ($T_{\rm peak}$=1.3 GK) of the hy-

drodynamic model 1 from Ref. [46]. For each of these histories, separate postprocessing calculations were performed using the previous rates from Görres *et al.* [13], Chen *et al.* [15], Matic *et al.* [18], He *et al.* [20], and the present rate; all other rates in the reaction network [44] were left unchanged. For brevity, we only discuss below the impact of the Görres *et al.* and present rates in the `K04` model. For both the `K04` and `S01` models, the rate of Matic *et al.* gave qualitatively similar results to those using the present rate; the rates from Refs. [15, 20] gave similar results to those using the rate of Görres *et al.*. Furthermore, no significant differences in either the nuclear energy generation rate or the final nucleosynthesis were observed when comparing results using any of the above rates with the profile extracted from Ref. [46].

As shown in Fig. 4, a striking difference in the nuclear energy generation rate at early times is seen when comparing XRB calculations using the present and Görres *et al.* rates. The nuclear energy generation rate increases by a factor of 1.8 between 0.3 to 0.35 s using the present rate. This also results in a dramatic change in the ^{18}Ne(α,p)^{21}Na reaction flux at these times. For example, at 0.35 s, the ^{18}Ne(α,p)^{21}Na reaction flux is increased by about a factor of 3. Our relatively larger new rate results in the depletion of ^{15}O and ^{18}Ne at early times by roughly a factor of 4 relative to abundances calculated using Görres *et al.* rate.

In addition, the ^{18}Ne(α,p)^{21}Na rate dominates over the β-decay of ^{18}Ne at an onset temperature of $T_9 \approx 0.47$ (assuming a typical XRB density of 10^6 g/cm^3) with the Matic *et al.* and present rates. This critical temperature is noticeably lower than the breakout temperature of $T_9 \approx 0.60$ determined using the rates from the work of Görres *et al.* and Chen *et al.* It implies that this reaction initiates the breakout earlier than previously thought.

Given the dramatic impact of the ^{18}Ne(α,p)^{21}Na rate on the nuclear energy generation rate in these postprocessing calculations, it is clear that similar tests using full hydrodynamic XRB models are urgently needed to examine these effects in detail. Such tests are already underway.

Acknowledgments

We would like to thank the RIKEN and CNS staff for their friendly operation of the AVF cyclotron. This work was financially supported by the National Natural Science Foundation of China (Nos. 11135005, 11021504), the Major State Basic Research Development Program of China (2013CB834406), as well as supported by the JSPS KAKENHI (No. 21340053). AP was supported by the Spanish MICINN (Nos. AYA2010-15685, EUI2009-04167), by the E.U. FEDER funds as well as by the ESF EUROCORES Program EuroGENESIS.

[1] W. Lewin, J.van Paradijs, R.E. Taam, Space Sci. Rev. **62**, 223 (1993).
[2] T. Strohmayer, L. Bildsten, in: W. Lewin, M. van der Klis (Eds.), Compact Stellar X-Ray Sources, Cambridge Univ. Press, 2006, p. 113.
[3] A. Parikh *et al.*, Prog. Part. Nucl. Phys. **69**, 225 (2013).
[4] S.E. Woosley and R.E. Taam, Nature **263**, 101 (1976).
[5] P.C. Joss, Nature **270**, 310 (1977).
[6] B. Lazareff *et al.*, Astrophys. J. **228**, 875 (1979).
[7] M. Wiescher *et al.*, J. Phys. G: Nucl. Part. Phys. **25**, R133 (1999).
[8] R.K. Wallace and S.E. Woosley, Astrophys. J. Suppl. **45**, 389 (1981).
[9] H. Schatz *et al.*, Phys. Rep. **294**, 167 (1998).
[10] S.E. Woosley *et al.*, Astrophys. J. Suppl. **151**, 75 (2004).
[11] H. Schatz *et al.*, Phys. Rev. Lett. **86**, 3471 (2001).
[12] V.-V. Elomaa *et al.*, Phys. Rev. Lett. **102**, 252501 (2009).
[13] J. Görres *et al.*, Phys. Rev. C **51**, 392 (1995).
[14] M. Wang, G. Audi, A.H. Wapstra *et al.*, Chin. Phys. C **36**(12), 1603 (2012).
[15] A.A. Chen *et al.*, Phys. Rev. C **63**, 065807 (2001).
[16] J.A. Caggiano *et al.*, Phys. Rev. C **66**, 015804 (2002).
[17] G.P.A. Berg *et al.*, Nucl. Phys. **A718**, 608 (2003).
[18] A. Matic *et al.*, Phys. Rev. C **80**, 055804 (2009).
[19] K.Y. Chae *et al.*, Phys. Rev. C **79**, 055804 (2009).
[20] J.J. He *et al.*, Phys. Rev. C **80**, 015801 (2009).
[21] W. Bradfield-Smith *et al.*, Phys. Rev. C **59**, 3402 (1999).
[22] D. Groombridge *et al.*, Phys. Rev. C **66**, 055802 (2002).
[23] P.J. Salter *et al.*, Phys. Rev. Lett. **108**, 242701 (2012).
[24] C. Ruiz *et al.*, Phys. Rev. C **71**, 025802 (2005).
[25] K.P. Artemov *et al.*, Sov. J. Nucl. Phys. **52**, 408 (1990).
[26] W. Galster *et al.*, Phys. Rev. C **44**, 2776 (1991).
[27] S. Kubono, Nucl. Phys. **A693**, 221 (2001).
[28] S. Kubono *et al.*, Eur. Phys. J. A **13**, 217 (2002).
[29] Y. Yanagisawa *et al.*, Nucl. Instr. Meth. A **539**, 74 (2005).
[30] T. Teranishi *et al.*, Phys. Lett. B **556**, 27 (2003).
[31] T. Teranishi *et al.*, Phys. Lett. B **650**, 129 (2007).
[32] J.J. He *et al.*, Phys. Rev. C **76**, 055802 (2007).
[33] H. Yamaguchi *et al.*, Phys. Lett. B **672**, 230 (2009).
[34] H. Yamaguchi *et al.*, Nucl. Instr. Meth. A **589**, 150 (2008).
[35] H. Kumagai *et al.*, Nucl. Instr. Meth. A **470**, 562 (2001).
[36] J.J. He *et al.*, *Origin of Matter and Evolution of Galaxies 2011*, Eds. S. Kubono *et al.*; AIP Conf. Proc. 1484, 240 (2012).
[37] Micron Semiconductor Ltd., Lancing, UK. http://www.micronsemiconductor.co.uk/.
[38] J.F. Ziegler *et al.*, *The Stopping and Range of Ions in Solids* (Pergamon Press, New York, 1985).
[39] M. Mukherjee *et al.*, Phys. Rev. Lett. **93**, 150801 (2004).
[40] A.M. Lane and R.G. Thomas, Rev. Mod. Phys. **30**, 257 (1958).
[41] R.O. Nelson, E.G. Bilpuch, and G.E. Mitchell, Nucl. Instr. Meth. A **236**, 128 (1985).
[42] L.Y. Zhang, J.J. He *et al.*, in preparation.
[43] T. Rauscher and F.-K. Thielemann, At. Data Nucl. Data Tables **75**, 1 (2000).
[44] A. Parikh *et al.*, Astrophys. J. Suppl. **178**, 110 (2008).
[45] A. Parikh *et al.*, Phys. Rev. C, **79**, 045802 (2009).
[46] J. José *et al.*, Astrophys. J. Suppl. **189**, 204 (2010).